

# Iris Segmentation and Recognition Using Enhance disocentric Segmentor and Wavelet Rectangular Coder

P.M. Siva Raja<sup>1</sup>, R.P. Sumithra<sup>2</sup>, S. Vidhya<sup>3</sup>

<sup>1,2,3</sup>Department of Computer Science & Engineering, Amrita College of Engineering and Technology, Nagercoil, India

\*\*\*

**Abstract** - An abstract summarizes, in one paragraph (usually), the major aspects of the entire paper in the following prescribed sequence. Iris based authentication system is essentially a pattern recognition technique that makes use of iris patterns, which are statistically unique, for the purpose of personal identification. In this paper, a novel method for improved iris recognition system with reduced false acceptance rate (FAR) and false rejection rate (FRR) using enhance disc centric segmentor (EISOS) and wavelet rectangular coder (WRC). The iris and pupil are very famous circular characteristics which are distinguished by an approximately stable intensity along the limbus (the junction between the sclera and the iris), and the iris and the pupil. In order to localize pupillary boundaries, the module of pupil segmentation is planned. At first, locate the Centre of the eye within the area of the pupil on low resolution images using EISOS method. In addition, EISOS gives an accurate eye center location in standard low resolution images with complete and fulfillment in segmentation structure. Once the iris region is successfully segmented from an eye image, the next stage is to transform the iris region into the fixed dimensions. After that, propose a new iris recognition system using a novel feature vector generation method namely, wavelet rectangular coder (WRC). The binary encoder based on texture feature is suitable to do iris recognition. It also, preserves the texture feature of the image by the neighborhood pixel replacement process for every block. Finally, recognize the iris image using fuzzy logic classifier which recognizes if the iris image is present in the dataset or not. Experimental results indicate that the proposed method of EISOS+WRC to iris segmentation and recognition framework have outperformed by having better accuracy of 99.75% when compared with existing approaches () that only achieved 94% and 93%.

**Key Words:** Segment, Wavelet rectangular coder, pattern recognition.(Minimum 5 to 8 key words)...

## 1.INTRODUCTION

The expression "Biometrics" refers to a science concerning the statistical analysis of biological characteristics. Over the last decade, Biometric authentication has been obtaining wide attention with growing demands in automated personal identification. To recognize individuals is the plan of biometrics by means of physiological or behavioral characteristics such as fingerprints, face, iris, retina and palm prints. Iris recognition is one of the most promising approaches among many biometric techniques, due to its

high dependability for personal identification. The iris is an interior organ of the eye. eyelashes, light reflections, shadows, etc. Thus, iris segmentation as well comprises localizing the eyelids and eradicating the effect of occlusions caused by the eyelashes, shadows and light reflections. In iris detection and recognition, feature extraction and selection are significant steps. An optimum feature set should have effectual and discriminating features, while mostly decreasing the redundancy of features pace to evade "curse of dimensionality" problem. Feature selection develops the precision of algorithms by decreasing the dimensionality and eliminating unrelated features.

Diverse classification methods from statistical and machine learning area have been used to iris recognition. Recognition is a fundamental task in data analysis and pattern recognition that needs the construction of classifiers. To identify the iris many machine learning techniques have been used together with support vector machine (SVM), Hear wavelet transform, k-nearest neighbor (k-NN), Baughman's algorithm, iris recognition by means of histogram analysis through LPQ and RI-LPQ method, Score Based Fusion Method, neural network, LBP and combined LBP classifier. In a number of applications such as organization and categorization, prediction, pattern recognition and control, neural networks model biological neural networks in the brain and have confirmed their competence. An artificial neural network contains intersected groups of artificial neurons. Such a network executes computation and organizes information based on the connectionist approach in a related however simpler fashion than the brain would execute. In addition, fuzzy logic is a kind of soft computing, which imitates human decision making, this classifier as well applied to identify the iris region.

## 2. PROPOSED SYSTEM

Iris based authentication system is essentially a pattern recognition technique that makes use of iris patterns, which are statistically unique, for the purpose of personal identification. In this paper, a novel method for recognition of iris patterns is considered by using a combination of Enhanced Isocentric Segmentor (EISOS), Wavelet Rectangular Coder (WRC) and fuzzy logic classifier. The flow diagram of proposed method is illustrated in figure 1. The first step of iris recognition is to extract the actual iris region in a digital eye image. To do this step, at first, pupil and iris

regions are segmented using enhanced isocentric segmentation (EISOS) method. The second step is to generate the Iris code feature vector and then to convert the circular to rectangular using Wavelet Rectangular Coder (WRC). In the final step, the iris recognition is done through fuzzy classifier.

### 3. PROBLEM DEFINITION AND DESCRIPTION

To control the access to limited places, modern security sciences use these differences which are one of the basic problems in security field. The rising necessitate of the security field has given go up to the development of current and competent authentication systems. In several application areas old approaches of recognition such as key or password are not suitable. These conventional techniques can be forgotten, stolen, or cracked. For these weaknesses, the current science is concerned in automatic systems of recognition which are based on biometrics technology. Into two major classes biometric identification is subdivided; physiological features such as fingerprints, iris and performance features such as voice. The necessitate of dependable and secure systems has engaged the emergence of the biometric system. Finger print, face and speaker recognition have been broadly studied. For authenticity check, among all the biometric recognition system (IRS) is the most competent and dependable system. Flam and Aram suggested Iris recognition. Current surveys of iris recognition algorithm can be found.

### 4. ARCHITECTURAL DESIGN

Iris based authentication system is essentially a pattern recognition technique that makes use of iris patterns, which are statistically unique, for the purpose of personal identification. In this paper, a novel method for recognition of iris patterns is considered by using a combination of Enhanced Isocentric Segmentor (EISOS), Wavelet Rectangular Coder (WRC) and fuzzy logic classifier. The architecture diagram of proposed method is illustrated in figure 4.1.

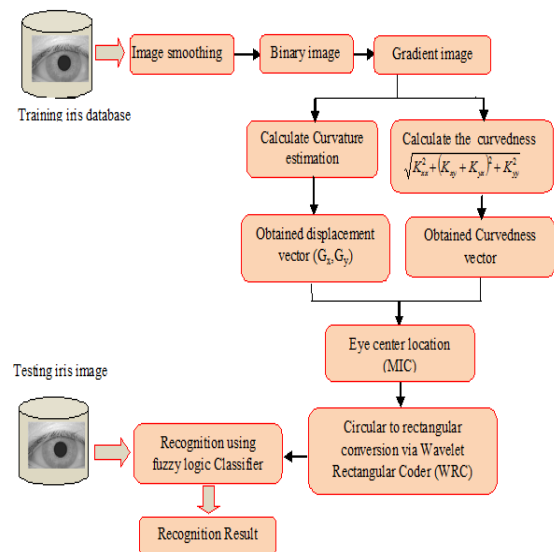


Fig -1: Architecture Diagram

The first step of iris recognition is to extract the actual iris region in a digital eye image. To do this step, at first, pupil and iris regions are segmented using enhanced isocentric segmentation (EISOS) method. The second step is to generate the Iris code feature vector and then to convert the circular to rectangular using Wavelet Rectangular Coder (WRC). In the final step, the iris recognition is done through fuzzy classifier.

#### 4.1 Segmentation

The iris and pupil are very famous circular characteristics which are distinguished by an approximately steady intensity along the limbus (the junction between the sclera and the iris), and the iris and the pupil. In order to localize pupillary boundaries the module of pupil segmentation is planned. More specifically, the module is responsible for performing the following four processing steps, namely: (i) image smoothing, (ii) binary image generation (binarization), (iii) Isophotes curvature estimation and (iv) pupil center and boundary localization. A detailed description of the pupil segmentation procedures involved in each step is given below. For the illustration purpose, Fig. 2 shows some major involved processing procedures and the obtained results through their respective sample iris image representations. Details in each step are covered in the remainder of this section.

##### 1) Stage 1: Image Smoothing

Consider the gray scale image  $K_{gray}$ , which have some of the noises; so we reduced the noise using smoothing methodology. Smoothing is often used to reduce noise with an image or to produce less pixilated image.

2) Stage 2: Binary image generation

Firstly, the iris image is converted into binary image, which means it converts an image of up to 256 gray levels to a black and white image. The grey level importance of every pixel in the improved image is considered in this stage. The input image is given a threshold value and categorizes all pixels with values above this threshold as white, and all other pixels as black in image binarization process. The binarization operation here mentioned aims at identifying and isolating some regions of interest in the raw input image from its background. The threshold value used for generating the desirable binary image is automatically estimated in advance from the gray level histogram of the improved image.

$$B_{Binary(i,j)} = \begin{cases} 0, & \text{if } K_{gray(i,j)} < \text{Threshold} \\ 1, & \text{Otherwise} \end{cases} \quad (1)$$

Where;

$B_{Binary}$  → Obtained binary image

$K_{gray}$  → Input gray scale image

3) Stage 3: Isophotes curvature estimation

To divider data is the purpose of segmentation so as to appear at significant areas. The boundary among areas is called an edge. The aim of this poster is to demonstrate the localization error of curved edges with often employed edge detection methods owing to the blurring effect. Now the blurring effect of the acquisition is modeled as the convolution with a point-spread function (PSF). In our effort, the first and second derivatives in the X direction of an image K are indicated as,  $K_x$  and  $K_{xx}$  correspondingly. The

existing algorithm is based on the study of the curvature of Isophotes, curves joining pixels in the image with equal intensity. The isophote curvature  $\delta$  is upright to the gradient and it is autonomous of the size of the gradient. Isophotes properties make them mainly appropriate for objects detection and image segmentation. In specific, it has been expressed that their shapes are independent of rotation and differing lighting conditions, and, in common, isophote features result in improved detection performance than intensities, gradients or Haar-like features.

To better illustrate the Isophotes framework, the notion of intrinsic geometry is introduced, i.e. geometry with a locally defined coordinate system. A local coordinate frame is set in every point of the image, in such a way that it spots in the direction of the maximal change of the intensity, which communicates to the direction of the gradient. This reference frame  $\{a, b\}$  is as well referred to as the gauge coordinates.

In a fixed coordinate system derivatives are worked out. The vector b is termed in the direction of the gradient and ais upright to b. Its frame vectors  $\hat{a}$  and  $\hat{b}$  are termed as:

$$\hat{b} = \frac{\{K_x, K_y\}}{\sqrt{K_x^2 + K_y^2}} \hat{a} = \perp \hat{b} \quad (2)$$

Where,  $K_x$  and  $K_y$  are the first order derivatives of the

luminance function  $K(x, y)$  in x and y dimension,

respectively. In this setting, a derivative in the b direction is the gradient itself, and the derivative in the a direction (perpendicular to the gradient) is 0 (no intensity change along the Isophotes). In this coordinate system the isophote is defined as  $K(a, b(a)) = \text{constant}$  and its curvature is

defined as the change  $\frac{d^2b}{da^2}$  of the tangent vector  $\frac{db}{da}$ . By implicit

differentiation with respect to a of the Isophotes definition, we obtain:

$$\frac{db}{da} K_b + K_a = 0; \quad \frac{db}{da} = -\frac{K_a}{K_b} \quad (3)$$

$$\frac{d^2b}{da^2} = -K_a K_b^{-1} \quad (4)$$

Since,  $K_a = 0$  from the gauge condition, then  $\frac{db}{da} = 0$ .

Therefore differentiating (3) once again respect to a, yields

$$\frac{d^2b}{da^2} = -K_{aa} K_b^{-1} - K_b^{-1} K_{ab} \frac{db}{da} + K_a K_b^{-2} \quad (4)$$

By consider the equation (3) we substitute the  $g = K_{bb} K_a = 0$  and recalling that  $\frac{db}{da} = 0$  the isophote curvature is obtained as

$$g = -\frac{K_{aa}}{K_b} \quad (5)$$

Substituting equation (3) into (4) yield,

$$\frac{d^2b}{da^2} = -K_{aa} K_b^{-1} + K_b^{-1} K_{ab} K_a K_b^{-1} + K_a K_b^{-2} K_{ba} - K_b^{-2} K_{bb} K_a K_b^{-1} = 0 \quad (6)$$

$$= -K_{aa} K_b^{-1} + K_{ab} K_a K_b^{-2} + K_{ba} K_a K_b^{-2} - K_a K_{bb} K_b^{-3} K_a \quad (7)$$

$$= -\frac{K_{aa} K_b^2}{K_b^2} + 2K_{ab} K_a K_b^{-2} - \frac{K_a^2 K_{bb}}{K_b^2} \quad (8)$$

The equation (8) in Cartesian coordinate it's given in equation (9).

$$g = -\frac{K_{aa}}{K_b} = -\frac{K_x^2 K_{yy} - 2K_x K_{xy} K_y + K_y^2 K_{xx}}{(K_x^2 + K_y^2)^{3/2}} \quad (9)$$

Where,  $\{K_x, K_y\}$  and  $\{K_{xx}, K_{yy}, K_{zz}\}$  are the first and second order derivatives of the luminance function  $K(x, y)$  in the x and y dimensions respectively. To better representation of the eye image, a simplistic eye model is used, shown in Figure 2, the isophote curvature of the eye model is shown in figure 3.

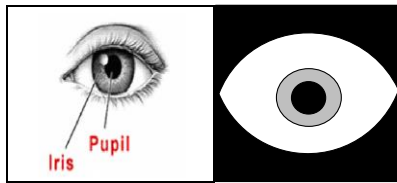


Fig -2: The original eye and notification of pupil and iris.

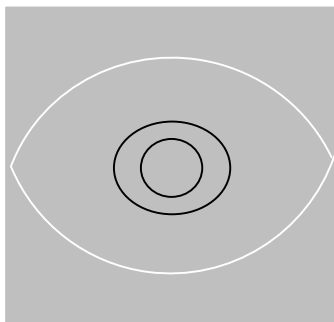


Fig -3: Isotopes curvature at the edges.

4) Stage 4: Center position estimation using displacement vector

After the isophote curvature estimation using section stage 3, we calculate the centre of the isophote in this section. For every pixel, we are interested in retrieving the center of the circle which fits the local curvature of the isophote. We make out the curvature is the reciprocal of the radius R; so equation (5) is turned around to attain the radius of this circle R.

$$R = \frac{1}{g} \quad (10)$$

The obtained radius magnitude is meaningless if it is not combined with orientation and direction. The orientation can be estimated from the gradient, but its direction will always point towards the highest change in the luminance as shown in figure 4. However, the sign of the isophote curvature depends on the intensity of the outer side of the curve (for a brighter outer side the sign is positive). Accordingly, by multiplying the gradient with the contrary of the isophote curvature, the sign of the isophote curvature

assists in disambiguating the direction to the center. As the unit gradient can be written as  $\frac{\{K_x, K_y\}}{K_b}$ , we contain

$$(G_x, G_y) = \frac{(K_x, K_y)}{K_b} \left[ -\frac{K_b}{K_{aa}} \right] = \frac{\{K_x, K_y\}}{K_{aa}} \quad (11)$$

$$= \frac{\{K_x, K_y\}(K_x^2 + K_y^2)}{K_y^2 K_{xx} - 2K_x K_{xy} K_y + K_x^2 K_{yy}} \quad (13)$$

Where  $\{G_x, G_y\}$  are the displacement vectors to the estimated position of the centers which can be mapped into an accumulator, hereinafter "center map". The set of vectors pointing to the estimated centers are shown in Figure 3(b). When compared to Figure 4 it is possible to note that the vectors are now all correctly directed towards the center of the circular structures. Figure 5.2 (c) represents the cumulative vote of the vectors for their center estimate (i.e. the accumulator). Since every vector gives a rough estimate of the center, the accumulator is convolved with a Gaussian kernel so that each cluster of votes will form a single center estimate. The contribution of each vector is weighted according to a relevance mechanism.

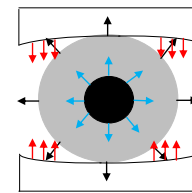


Fig -4: The direction of the gradient under the image's edges.

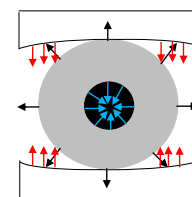


Fig -5: The displacement vectors pointing to the isophotes centers.

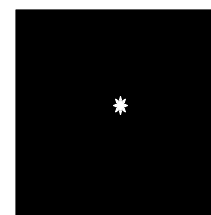


Fig -6: The center map.

5) Stage 5: Centre voting and eye center location

Reflect on the figure 3(a), we employing only three Isophotes; one explaining the pupil, one explaining the iris

and final one explaining the boundary of the sclera. By convolving the eye model with Gaussian kernel, it can be examined that the number of isophotes raises around the edges as the steepness of the edge reduces, and that each of these novel isophotes is same to the original isophotes thus we employ to produce additional evidence to vote for right centre. The discretization problem in a digital image could be diminished and invariant and precise eye centre estimation could be attained by gathering and averaging local evidence of curvature. To this conclusion, an image operator that points out how much a region diverges from flatness is required. This operator is the curvedness, termed as

$$Curvedness = \sqrt{L_{xx}^2 + (L_{xy} + L_{yx})^2 + L_{yy}^2} \quad (12)$$

The curvedness is regarded as a rotational invariant gradient operator, which calculates the degree of steepness of the gradient. As a result, it gives up low response on flat surfaces and edges, while it yields high response around the edges. As isophotes are slices of the intensity landscape, there is a straight relation among the value of the curvedness and the density of isophotes. As a result, denser isophotes are possible to belong to the similar feature (i.e. edge) and hence locally agree on the similar center. By summing the votes by means of equation (5), we attain high responses around the center of isocentric Isophotes patterns. We name these high responses “isocenters”, or ICs. The maximum isocenter (MIC) in the centermap will be employed as the most possible estimate for the sought after position of the center of the eye.

The MIC is calculated based upon the following condition:

$$MIC = \begin{cases} C(i, j) & \text{if } G_x(i, j), G_y(i, j) > 0 \\ & \text{and} \\ 0 & \text{if } G_x(i, j), G_y(i, j) = T_l, T_l = L_B \text{ to } U_B \\ & \text{otherwise} \end{cases} \quad (13)$$

Where,

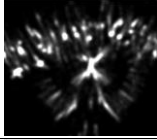
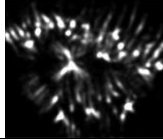
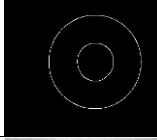
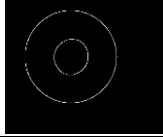
$G_x(i, j) \rightarrow$  Displacement vector at x direction

$G_y(i, j) \rightarrow$  Displacement vector at y direction

The intermediate steps of the MIC determination are presented in table 1 to better understanding the concept clearly.

**Table -1:** The intermediate steps of the MIC determination

Steps	Image 1	Image 2
Input		

Obtained centre map		
The edges that contributed to the vote of the MIC		
Segmented output		

#### 4.2 Feature extraction

Once pupil and iris regions are segmented using EISOS method, the feature extraction is performed using Wavelet Rectangular Coder (WRC) algorithm. At first, Daugman’s Rubber Sheet Model is used to convert circular to rectangular conversion (CTRC) operation. Here, the iris area i.e. polar coordinate is converted Cartesian coordinates. Therefore, iris area is obtained as a normalized strip with regard to iris boundaries and pupillary center. The homogenous rubber sheet model is an efficient normalization method, which is devised by Daugman (1993) used for normalization process. The rectangular iris image with size of  $M \times N$  is then applied for the code generation process using WRC (Wavelet Rectangular Coder) method. In order to design this, n-level of wavelet decomposition is done based on the input image and the designed rectangular operator and iris code is generated based on nth level wavelet co-efficient. The detailed process of the feature extraction scheme is presented in this subsection:

##### 1) Daugman’s Rubber Sheet Model:

Normalization process includes un-wrapping the iris and transforming it into its polar equivalent. It is performed utilizing Daugman’s Rubber sheet model and is depicted in the following figure 7, on polar axes, for each pixel in the iris, its equivalent position is found out. The process consists of two resolutions: (i) Radial resolution and (ii) Angular resolution. The former is the number of data points in the radial direction whereas, the later part is the number of radial lines produced around iris region. Utilizing the following equation, the iris region is transformed to a 2D array by making use of horizontal dimensions of angular resolution and vertical dimension of radial resolution.

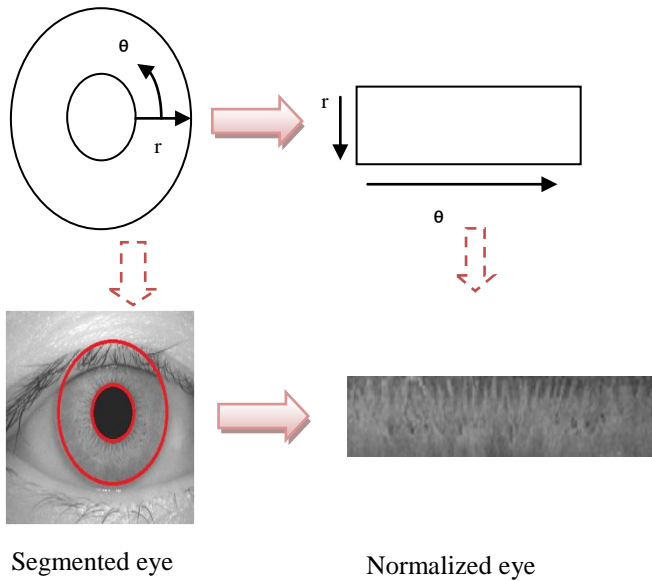


Fig -7: Daugman's Rubber Shett Model.

$$I[x(r, \theta), y(r, \theta)] \rightarrow I(r, \theta) \quad (16)$$

Where,  $I(x, y)$  is the iris region,  $(x, y)$  and  $(r, \theta)$  are the Cartesian and normalized polar coordinates respectively. The range of  $\theta$  is  $[0, 2\pi]$  and  $r$  is  $[0, 1]$ .  $x(r, \theta)$  and  $y(r, \theta)$  are described as linear combinations set of pupil boundary points. To perform the transformation, the formulas are given in the preceding equations

$$\begin{aligned} x(r, \theta) &= (1 - r)x_p(\theta) + x_i(\theta) \\ y(r, \theta) &= (1 - r)y_p(\theta) + y_i(\theta) \\ x_p(\theta) &= x_{p0}(\theta) + r_p \cos(\theta) \\ y_p(\theta) &= y_{p0}(\theta) + r_p \sin(\theta) \\ x_i(\theta) &= x_{i0}(\theta) + r_i \cos(\theta) \\ y_i(\theta) &= y_{i0}(\theta) + r_i \sin(\theta) \end{aligned} \quad (14)$$

Where,  $(x_p, y_p)$  and  $(x_i, y_i)$  are the coordinates on the pupil and iris boundaries along the  $\theta$  direction.  $(x_{p0}, y_{p0}), (x_{i0}, y_{i0})$  are the coordinates of pupil and iris centers. This model gives a rectangular array with size of  $M \times N$  image to generate binary code to form feature set.

## 2) Wavelet Rectangular Coder (WRC)

Once CTCRC operation is done via Daugman's Rubber Sheet Model, the code generation process is performed using Wavelet Rectangular Coder (WRC) algorithm. To effectiveness of the feature extraction stage, a novel algorithm is proposed called as Wavelet Rectangular Coder (WRC) to remove or process that corrupted iris parts based on the quality assumption. At first, wavelet transform is

applied to the normalized iris image. Generally, wavelets can be used to analyze the data in the iris region in multi-resolution mode. Wavelets have the advantage over traditional Fourier transform as the frequency data is localized in wavelet, allowing features which occur at the same position and resolution to be matched up. The step by step process of WRC algorithm is given below;

Let the original image (rectangular array) be denoted as  $A(x, y)$ ,

- the LL band transformation image be denoted as  $A_{LL}(x, y)$ ,
- HL band transformation image be denoted as  $A_{HL}(x, y)$ ,
- the LH band transformation image be denoted as  $A_{LH}(x, y)$
- the HH band transformation image be denoted as  $A_{HH}(x, y)$
- The binary code of  $A_{LL}(x, y)$  denoted as  $BC_{LL}$ ,
- the binary code of  $A_{HL}(x, y)$  is denoted as  $BC_{HL}$ ,
- the binary code of  $A_{LH}(x, y)$  is denoted as  $BC_{LH}$  and
- binary code of  $A_{HH}(x, y)$  is denoted as  $BC_{HH}$ .

The obtained single 8-bit binary code is denoted as  $B_S$  and the corresponding decimal value is denoted as  $D_B$ . The final output of the rectangular array image is represented as  $A_{out}(x, y)$ .

b) At first, the DWT is applied and decomposed into Fourier sub bands like LL, HL, LH, and HH. Subsequently, each sub bands are divided into set of blocks. Here, a set is represented as  $3 \times 3$  blocks with centre pixel

c) The main intention is to code generation from these each  $3 \times 3$  blocks to replace center pixel in the original image. To do this process, one condition is applied on each centre block based on each neighborhood to generate 8-bit binary code. The condition is given as follows:

$$P_i = \begin{cases} 1 & \text{for } X_i > X_c \\ 0 & \text{for otherwise} \end{cases} \quad (15)$$

Where,

$$P_i \rightarrow i^{th} \text{ Pixel}$$

$$X_c \rightarrow \text{Center block of the } 3 \times 3 \text{ block}$$

$$X_i \rightarrow i^{th} \text{ block}$$

d) After this condition, 8-bit binary code is generated for each 3\*3 blocks in every sub bands. Mathematically, the binary code generation can be represented as

$$BC_{LL} \leftarrow [A_{LL}(x, y)]_{3 \times 3}$$

$$BC_{HL} \leftarrow [A_{HL}(x, y)]_{3 \times 3}$$

$$BC_{LH} \leftarrow [A_{LH}(x, y)]_{3 \times 3}$$

$$BC_{HH} \leftarrow [A_{HH}(x, y)]_{3 \times 3}$$

e) After the binary code conversion, the OR operation is performed to obtain single 8-bit binary code

$$B_s = OR[BC_{LL}, BC_{HL}, BC_{LH}, BC_{HH}]$$

f) Finally, the single 8-bit binary code is converted to equal decimal value and consider as the value of the central pixel value. The above process is repeated for whole image to obtain  $A_{out}(x, y)$ .

g) Finally, column-wise mean value is taken for obtained  $M \times N$  image, and it is deducted to size of  $1 \times N$  and it gives to recognition phase. The figure 8 illustrates the numerical example of the WRC process.

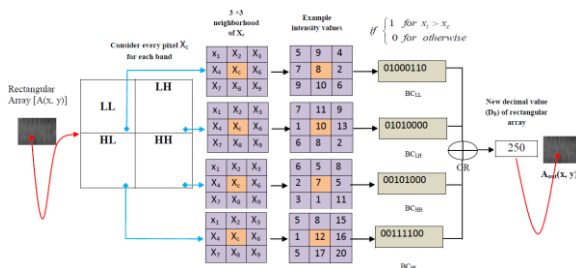


Fig - 8: Example process of the Wavlet Rectangular Coder (3RC).

### 4.3 Recognition

We have applied a fuzzy logic system using subtractive clustering for the recognition samples. The step by step process is explained below:

#### 1) Membership Function

In this model, the subtractive clustering is used to design membership function in input and output data points. In addition, the fuzzy rules are generated using subtractive clustering. Here, rule should have two different decisions like as YES and NO. From the rule set, sample rules are presented in table 2:

Table -2: Sample rule of the system

Rules	Sample Rules
copy	More table copya
R <sub>1</sub>	IF (X1 is C1) and (X2 is C1) and (X3 is C2) and (X4 is C1) and . . . (XN is C2) THEN Y0 =1
R <sub>2</sub>	IF (X1 is C2) OR (X2 is C1) OR (X3 is C1) OR (X4 is C2) OR . . . (XN is C1) THEN Y0=0.
.	.
.	.
.	.
R <sub>k</sub>	IF (X1 is C1) OR (X2 is C2) OR (X3 is C2) OR (X4 is C1) OR . . . (XN is C2) THEN Y0 =0

Where; R1, R2 . . . Rk are the fuzzy rules, X1, X2, X3. XN are the input attribute of the rectangular array with size  $1 \times N$ . C1 and C2 are the clusters. Y0 is 1 means recognized and Y0 is 0 means not recognized.

The recognition of iris sample is carried out using the fuzzy system designed in the previous sub-section. The testing iris image  $T_s$  is given to the fuzzy logic system, where the test iris image  $T_s$  is converted to the fuzzified value based on the fuzzy membership function. Then, the fuzzified input is matched with the fuzzy rules defined in the rule base. Here, the rule inference procedure is used to obtain the linguistic value that is then converted to the fuzzy score using the average weighted method. From the fuzzy score obtained, the decision is generated whether the test iris image belongs to the recognition or not. The figure 9 illustrates the Flow diagram of Genfis2 based

Fuzzy Interference System.

#### Interference System

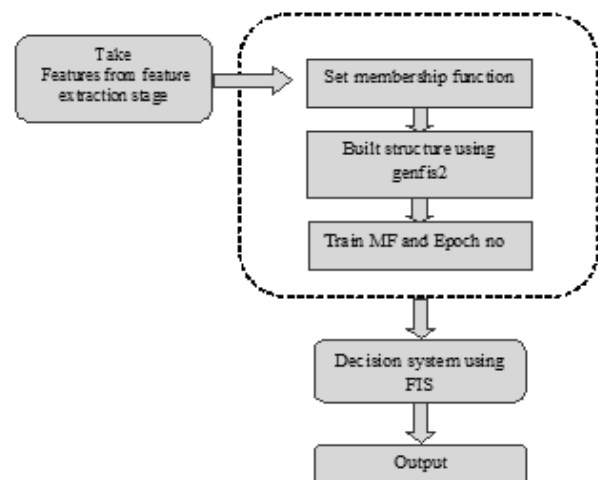


Fig - 9: Flow Diagram of Genfis2 based Fuzzy Interference System

## 5. TEST DATA AND RESULTS

In this section we discuss the result obtained from the propose technique. For implementing the propose technique we have used python This proposed technique is done in windows machine having Intel Core i5 processor with speed 1.6 GHz and 4 GB RAM. For comparing the performance, we using three type of dataset such as CASIA, UBRIS and MMU iris image database.

### 5.1 Evaluation Metrics

The evaluation of proposed iris recognition technique in bench mark iris image database are carried out using the following metrics as suggested by below equations,

**1)Accuracy:** The Accuracy of the proposed method is the ratio of the total number of TP and TN to the total number of data.

$$Accuracy = \frac{TN + TP}{(TN + TP + FN + FP)}$$

Where,

FP stands for false positive,

TP stands for true positive,

TN stands for true negative,

FN stands for false negative

- False Acceptance Rate (FAR): FAR is the probability rate at which numbers of Iris images are erroneously received as “non-match.
- False Rejection Rate (FRR): FRR is the probability rate at which the numbers of iris images are erroneously received as match.

### 2) Error Message

- If the login password is incorrect it will display error message
- In Segmentation, if the selected file is not a python file the error message will be displayed in the screen.
- In Feature extraction, if the selected file is not a python file, it displays
- An error message
- In the recognition, either the starting position or the ending position is not given, it will display error message.

### 3) Performance Results of peak Signals to Noise Ratio

Peak Signal to Noise Ratio (PSNR) is computed based on the mean square error which is defined as the difference between noisy image and preprocessed image. The mean square error and peak signal to noise ratio is computed as follows,

$$mse = (i_o - i_p)^2 \tag{16}$$

$$PSNR = 10 * \log_{10} \frac{r^2}{mse} \tag{17}$$

**Table-3:** Peak Signal to Noise Ratio versus Image Size

Brain Image size (KB)	Peak signal to noise ratio (dB)		
	LFBCR-EGB	Automatic and Data-Driven Procedure	PNN
23.1	36.53	34.50	33.97
21.7	42.55	40.17	38.30
23.0	46.54	38.02	36.53
21.9	44.04	38.58	36.76
24.6	47.30	43.52	39.18
23.7	49.04	41.68	36.30
25.0	46.54	40.17	33.81
24.4	54.15	46.54	44.04
31.8	52.56	48.13	43.52
38.4	45.85	42.55	39.83

The above table value clearly shows that the simulation results of peak signal to noise ratio with respect to different image sizes. The various MRI images are collected from the database. The performance of the peak signal noise ratio of the proposed LFBCR-EGB technique is significantly improved when compared to the existing Automatic and Data-Driven Procedure [1] and PNN [2]. The simulation graph with various results is shown in figure 10.

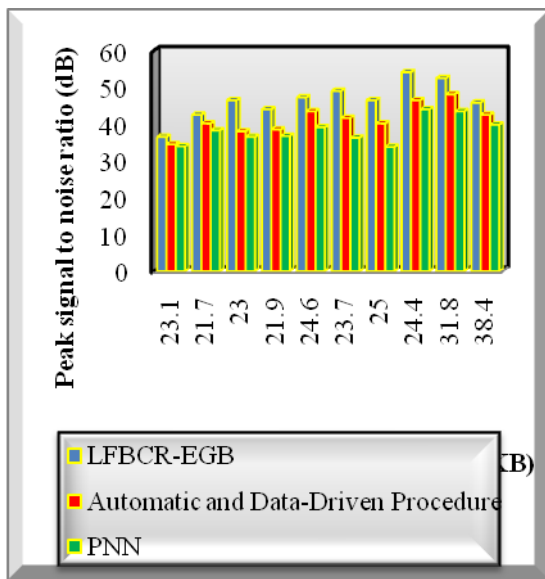


**Fig-10:** Simulation Results of Peak Signals to Noise Ratio

Figure 10 illustrates the simulation results of the peak signal to noise ratio based on the various image size from 23.1 KB-38.4 KB. The image size is taken as input in 'x' direction and the corresponding results of the peak signal to noise ratio are attained in 'y' direction. The above simulation result clearly shows that the proposed LFBCR-EGB technique increases the performance results of PSNR when compared to existing methods. This is because, proposed LFBCR-EGB technique removes the noises in an MRI image through the preprocessing steps. The LFBCR-EGB technique uses the weighted lee filter. This PSNR is computed by estimating the mean square error between the original size and quality enhanced image. The original images have a few noisy pixels to minimize the image quality for lesion localization. The weighted lee filter monitors the pixel in the images and its adjacent pixels. The entire pixels in an image are arranged in ascending order and find the center pixels and modified the all the pixels along with the center pixels. The center pixels in a window remove the noisy pixels. As a result, the peak signal to noise ratio gets improved.

## 6. CONCLUSION

The objective of this research was to demonstrate iris image segmentation and recognition. Here we have introduced a new method namely, iris segmentation recognition using EISOS+ WRC approach. Here, first the iris image was segmented using the enhanced isocentric segmentor (EISOS) method. After the segmentation we convert the segmented image into the rectangular coordinates using the Daugman's Rubber Sheet Model. Once we convert the rectangular coordinates, the code generation process is performed using Wavelet Rectangular Coder (WRC) algorithm. Finally, the fuzzy logic classifier is used to recognize the iris image using the fuzzy rules. The iris recognition performance is measured using different dataset such as, CASIA, MMU and UBIRIS dataset. Experimental results indicate that the

proposed method of EISOS+WRC to iris segmentation and recognition framework have outperformed by having better accuracy of 99.75.9% when compared with existing approach only achieved 94% and 93%.

## REFERENCES

- [1] J. Wayman, A. Jain, D. Maltoni, and D. Maio, "Biometric Systems", Springer, 2005.
- [2] L. Ma, T. Tan, Y. Wang, and D. Zhang, "Efficient Iris Recognition by Characterizing Key Local Variations", IEEE Trans. Image Processing, vol.13, No. 6, pp.739-750, June 2004.
- [3] C. Tisse, L. Martin, L. Torres, and M. Robert, "Person Identification Technique Using Human Iris Recognition", Proc. 15th Int'l Conf. Vision Interface, pp. 294-299, 2002.
- [4] Samir Shah and Arun Ross, "Iris Segmentation Using Geodesic Active Contours", IEEE transactions on information forensics and security, vol. 4, No. 4, 2009.
- [5] J. Daugman, "High-Confidence Visual Recognition of Persons by a Test of Statistical Independence", IEEE Trans. Pattern Analysis and Machine Intelligence, vol. 15, No. 11, pp. 1148-1161, Nov. 1993.
- [6] W. Boles and B. Boashash, "A Human Identification Technique Using Images of the Iris and Wavelet Transform", IEEE Trans. Signal Processing, vol. 46, No. 4, pp. 1185-1188, Apr. 1998.
- [7] J. Daugman, "New methods in iris recognition", IEEE Trans. Syst. Man Cybern Part B-Cybern., vol.37, pp. 1167-1175, 2007.
- [8] Alireza Osareh and Bitia Shadgar, "A Computer Aided Diagnosis System for Breast Cancer", IJCSI International Journal of Computer Science Issues, Vol. 8, No.2, 2011.
- [9] Karabatak, M., Ince, M.C., "An expert system for detection of breast cancer based on association rules and neural network", Expert Systems with Applications, Vol.36, pp.3465-3469, 2009.

## BIOGRAPHIES



**Dr. P.M. Siva Raja** present research interests include **Machine Learning in medical image processing** and information security in image processing. He is currently working as Assistant Professor at **Amrita College of Engineering and Technology**, Amritagiri, Kanyakumari District.



**Mrs. R.P. Sumithra** pursuing her research in **Computer aided medical image using Deep Learning techniques**. She is currently working as Assistant Professor at **Amrita College of Engineering and Technology**, Amritagiri, Kanyakumari District



**Mrs. S. Vidhya** received her M.E degree from the Department of CSE, Anna University, Chennai in 2012, her B.E degree from the Department of CSE, Anna University, Chennai in 2010. He is currently working as Assistant Professor at **Amrita College of Engineering and Technology**, Amritagiri, Kanyakumari District.